

Cite this: *Green Chem.*, 2012, **14**, 771

www.rsc.org/greenchem

PAPER

## Preparation of clay-supported Sn catalysts and application to Baeyer–Villiger oxidation†

Takayoshi Hara, Moriaki Hatakeyama, Arum Kim, Nobuyuki Ichikuni and Shogo Shimazu\*

Received 11th November 2011, Accepted 16th December 2011

DOI: 10.1039/c2gc16437j

Clay-intercalated Sn catalysts were prepared by a conventional cation-exchange method and used for the Baeyer–Villiger oxidation of various ketones with hydrogen peroxide as an oxidant. The intercalation of monomeric Sn species into the clay interlayer was monitored by solid-state  $^7\text{Li}$  MAS NMR. Solid-state  $^{119}\text{Sn}$  MAS NMR and Sn K-edge XAFS analysis revealed that an isolated Sn species, such as  $[\text{Sn}^{\text{IV}}(\text{OH})_x(\text{H}_2\text{O})_{5-x}]^{(4-x)+}$  ( $x = 0-3$ ), was formed in the clay interlayers. Our clay-intercalated Sn catalysts showed extremely high performance in Baeyer–Villiger oxidation and were also reusable without any significant loss of activity or selectivity.

## Introduction

The Baeyer–Villiger oxidation is the most widely applied reaction in organic synthesis.<sup>1</sup> Through this oxidation reaction, a variety of carbonyl compounds, such as ketones, cyclic ketones, benzaldehydes, and carboxylic acids, can be transformed into various oxidised products, such as esters, lactones, phenols, and anhydrides, respectively.<sup>2</sup> Although many types of homogeneous, heterogeneous, and enzyme catalysts have been reported for the Baeyer–Villiger oxidation, the reactions using these catalysts are often carried out with expensive, hazardous peracids, including *in situ* generated organic peroxides formed from aldehydes and molecular oxygen, leading to the formation of one equivalent of the corresponding carboxylic acid.<sup>3</sup> From the viewpoint of green and sustainable chemistry, many attempts to develop a heterogeneous catalytic system with hydrogen peroxide as the sole oxidant have been made.<sup>4</sup>

In 2001, Corma and his co-workers reported that Sn-containing beta zeolite (Sn- $\beta$ -zeolite) has become one of the most effective catalysts for the Baeyer–Villiger oxidation reaction with hydrogen peroxide.<sup>5a</sup> Based on the analyses using various characterisation techniques, it was revealed that the Lewis acidity of isolated tetrahedral  $\text{Sn}^{\text{IV}}$  species activates the carbonyl group of substrates. In addition, various types of heterogeneous catalysts, including Sn species such as Sn-dendrimer/polystyrene,<sup>6a</sup> Sn-MCM-14,<sup>6b</sup> Sn/cellulose,<sup>6c</sup> Sn/polystyrene,<sup>6d</sup> and Sn-containing clay minerals such as hydrotalcite,<sup>6e</sup> palygorskite,<sup>6f</sup> and montmorillonite,<sup>6g</sup> have been developed in the past decade.

Lithium taeniolite (Li/TN) of fluorotaeniolite type mica is composed of negatively charged layers between which there are lithium cations. The structure of Li/TN is built by stacking complex layers made of two  $\text{SiO}_4$  octahedral sheets and one  $(\text{Mg,Li})\text{O}_6$  octahedral sheet.<sup>7</sup> These stacked layers are connected with interlayer sheets made up of exchangeable  $\text{Li}^+$  cations and water molecules in the Li/TN matrix. With Li/TN as a host compound, we have already reported that various intercalated metal complex catalysts selectively promote various organic transformations.<sup>8</sup> In particular, TN-intercalated zirconium complexes efficiently catalyzed the ring-opening reaction of terminal oxiranes with various alcohols and carboxylic acids because of their Lewis acidity.<sup>8d,e</sup> We are now focusing on designing high-performance heterogeneous catalysts with isolated and uniform active species by a simple cation-exchange reaction between the clay host and interlayer guest cations.

In this paper, we wish to present the synthesis and characterisation of a TN-intercalated Sn catalyst and its evaluation as a heterogeneous catalyst for the Baeyer–Villiger oxidation of cyclic ketones using aqueous hydrogen peroxide. The highly dispersed isolated  $\text{Sn}^{\text{IV}}$  species in the TN interlayer has proven to be effective as a catalytically active species for selective and environmentally benign Baeyer–Villiger oxidation.

## Results and discussion

The chemical composition of Li/TN is ideally  $\text{Li}[(\text{Mg}_2\text{Li})(\text{Si}_4\text{O}_{10})\text{F}_2]$  and its cation exchange capacity (CEC) is 268.2 meq/100 g. Intercalation of Sn species into TN interlayers was achieved by a simple cation exchange process using  $\text{SnCl}_2 \cdot 2\text{H}_2\text{O}$  as a precursor.  $\text{SnCl}_2 \cdot 2\text{H}_2\text{O}$  is able to dissolve into a  $\text{CH}_3\text{OH}$ /water solution, giving a clear, colourless solution. In general, tin cations are easily transformed into insoluble tin hydroxide in water *via* hydrolysis of coordinated water molecules, because of its high Lewis acidity. It might be said that the hydrolysis, which leads to the formation of insoluble tin

Department of Applied Chemistry and Biotechnology, Graduate School of Engineering Chiba University, 1-33 Yayoi, Inage, Chiba 263-8522, Japan. E-mail: shimazu@faculty.chiba-u.jp; Fax: +81-43-290-3379; Tel: +81-43-290-3379

†Electronic supplementary information (ESI) available. See DOI: 10.1039/c2gc16437j

**Table 1** Results of chemical analyses of Sn(X)/TN catalysts

Catalyst	$d_{001}$ (degree)	BS (nm) <sup>a</sup>	CS (nm) <sup>b</sup>	LA (mmol g <sup>-1</sup> ) <sup>c</sup>
Li/TN	7.36	1.20	0.24	—
Sn(0.19)/TN	7.20	1.23	0.27	0.19
Sn(0.40)/TN	5.98	1.48	0.52	0.40
Sn(0.77)/TN	5.84	1.51	0.55	0.77

<sup>a</sup> Basal spacing. <sup>b</sup> Clearance space = BS – thickness of layer (0.96 nm).<sup>c</sup> Loading amount of Sn species determined by ICP analysis.

hydroxide, is inhibited by the addition of CH<sub>3</sub>OH, and a stable Sn complex is formed.

Three classes of TN-intercalated Sn catalysts are synthesised by varying the Sn loading amount (0.19, 0.40, or 0.77 mmol g<sup>-1</sup>), and the result of the chemical analysis are shown in Table 1. The synthesised catalysts are denoted Sn(X)/TN (the number in parentheses indicates the loading amount of the Sn species in mmol g<sup>-1</sup>). Powder X-ray diffraction (XRD) profiles revealed that Sn(0.19)/TN and the parent Li/TN had almost the same layered structures, and their CS values (clearance space = basal spacing – thickness of layer (0.96 nm)) were 0.27 and 0.24 nm, respectively.<sup>9</sup> The CS increased with increasing loading amount of Sn species, and Sn(0.77)/TN catalyst had a CS of up to 0.55 nm.

To confirm the progress of the cation exchange reaction, the TN-intercalated Sn catalysts were analysed by <sup>7</sup>Li magic-angle-spinning (MAS) nuclear magnetic resonance (NMR) (Fig. 1). Because of its high gyromagnetic ratio,  $\gamma(^7\text{Li})/\gamma(^1\text{H}) = 0.389$ , and its natural abundance (92.58%), <sup>7</sup>Li is a powerful probe for experimental studies exploiting this NMR technique.<sup>10</sup> Moreover, <sup>7</sup>Li is very sensitive to the asymmetry of its electrostatic environment because of its quadrupolar nucleus with 3/2 spin.<sup>11</sup> The chemical shift was referenced to LiCl as an external standard

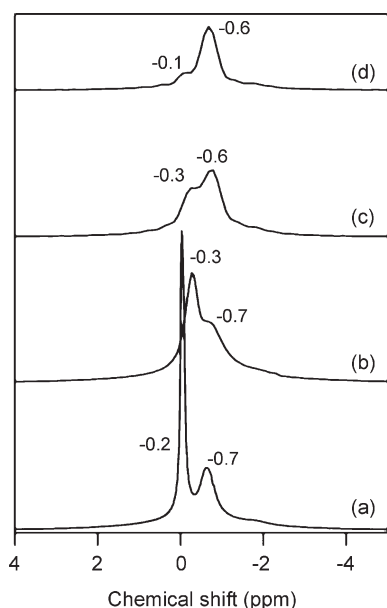


**Fig. 1** <sup>7</sup>Li MAS NMR spectra of (a) Li/TN, (b) Sn(0.19)/TN, (c) Sn(0.40)/TN, and (d) Sn(0.77)/TN catalyst, collected at a spinning rate of 20 kHz.

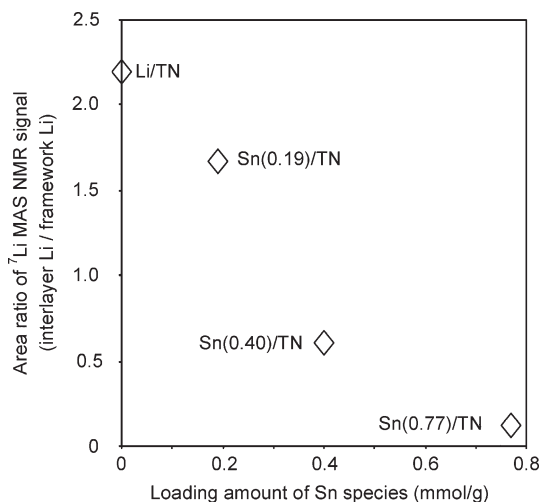


**Fig. 2** Relation between <sup>7</sup>Li MAS NMR signal and loading amount of Sn species.

(0 ppm). As can be clearly observed, two peaks at -0.2 and -0.7 ppm appeared in the spectrum of a Li/TN sample (Fig. 1a). This result strongly supports the Li<sup>+</sup> cations situate themselves at two crystallographic sites, *i.e.*, the Li<sup>+</sup> cations exist as exchangeable interlayer Li<sup>+</sup> cations and framework Li<sup>+</sup> cations in an octahedral sheet, as reported by Toraya and coworkers.<sup>7</sup> With the intercalation of the Sn species, the intensity of the peak at -0.3 ppm decreased slightly (Fig. 1b–d). For the results of <sup>7</sup>Li MAS NMR, it should be noted that the peaks around -0.2 and -0.6 ppm correspond to the interlayer exchangeable Li<sup>+</sup> cations and the framework Li<sup>+</sup> cations in the octahedral sheets, respectively.<sup>12</sup> The area ratio of the interlayer Li<sup>+</sup> peak to the framework Li<sup>+</sup> peak in the <sup>7</sup>Li MAS NMR spectra is inversely proportional to the loading amount of Sn species (Fig. 2), indicating the intercalation of Sn species into a TN interlayer occurs *via* a cation exchange reaction.

The local structure of Sn species in the TN interlayer was investigated with <sup>119</sup>Sn MAS NMR and Sn K-edge X-ray absorption fine structure (XAFS) spectroscopy. It is well known that there are three Sn isotopes: <sup>115</sup>Sn (0.35%), <sup>117</sup>Sn (7.67%), and <sup>119</sup>Sn (8.58%), which all possess a nuclear spin of 1/2.<sup>13</sup> In particular, <sup>119</sup>Sn NMR signals are detectable owing to the large sensitivity associated with the spin 1/2 of the <sup>119</sup>Sn nucleus.<sup>14</sup> The chemical shift was referenced to (CH<sub>3</sub>)<sub>4</sub>Sn as an external standard (0 ppm). For the crystalline SnO<sub>2</sub> sample (Fig. 3a), there was one sharp resonance at -604 ppm, in accordance with the cassiterite structure, in which there is one Sn site per unit cell and Sn<sup>IV</sup> is in almost regular octahedral surroundings.<sup>15,16</sup> The spectrum of the SnO sample is made up of many peaks because of the very strong Sn–Sn coupling constant (Fig. 3b).<sup>16</sup> In the case of TN-intercalated Sn catalysts, a broad peak at -604 ppm was observed (Fig. 3c–e), suggesting that the Sn species in the TN interlayer do not have the same structure as bulk SnO<sub>2</sub> but instead have a different distribution of Sn–O coordination numbers, bond angles, and bond lengths. Furthermore, the broad signals of TN-intercalated Sn catalysts might be due to various factors, such as a low concentration and the crystallinity of Sn species or the different natures of substituents of Sn.

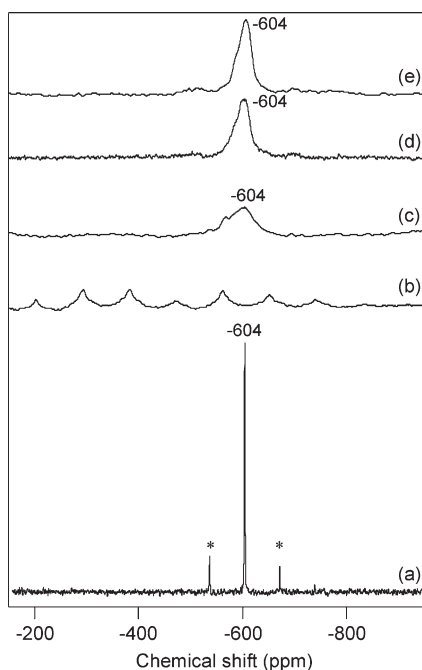


**Fig. 3**  $^{119}\text{Sn}$  MAS NMR spectra for (a)  $\text{SnO}_2$ , (b)  $\text{SnO}$ , (c)  $\text{Sn}(0.77)/\text{TN}$ , (d)  $\text{Sn}(0.40)/\text{TN}$ , and (e)  $\text{Sn}(0.19)/\text{TN}$  catalyst, collected at a spinning rate of 20 kHz. The asterisk denotes spinning sidebands.

In the Sn K-edge X-ray absorption near-edge structure (XANES) spectrum, the edge energy of the TN-intercalated Sn catalysts did not resemble that of  $\text{SnCl}_2 \cdot 2\text{H}_2\text{O}$  or  $\text{SnO}$  but were similar to those of  $\text{SnCl}_4 \cdot 5\text{H}_2\text{O}$  and  $\text{SnO}_2$  (Fig. 4). This similarity suggests that tetravalent Sn species are present in the TN interlayer. The Fourier transform (FT) of the  $k^3$ -weighted Sn K-edge extended X-ray absorption fine structure (EXAFS) data is

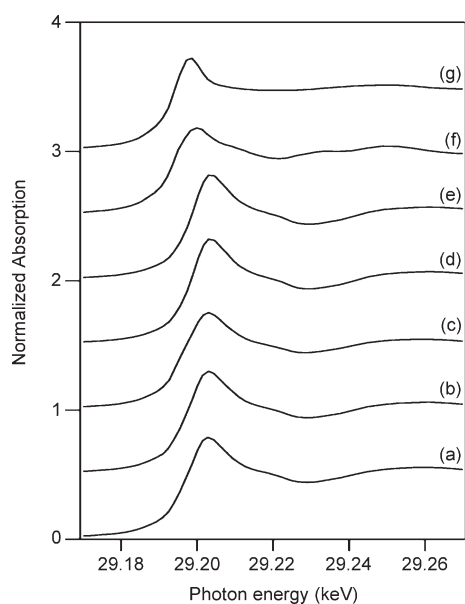


**Fig. 4** Sn K-edge XANES spectra for (a)  $\text{Sn}(0.19)/\text{TN}$ , (b)  $\text{Sn}(0.40)/\text{TN}$ , (c)  $\text{Sn}(0.77)/\text{TN}$ , (d)  $\text{SnO}_2$ , (e)  $\text{SnCl}_4 \cdot 5\text{H}_2\text{O}$ , (f)  $\text{SnO}$ , and (g)  $\text{SnCl}_2 \cdot 2\text{H}_2\text{O}$ .

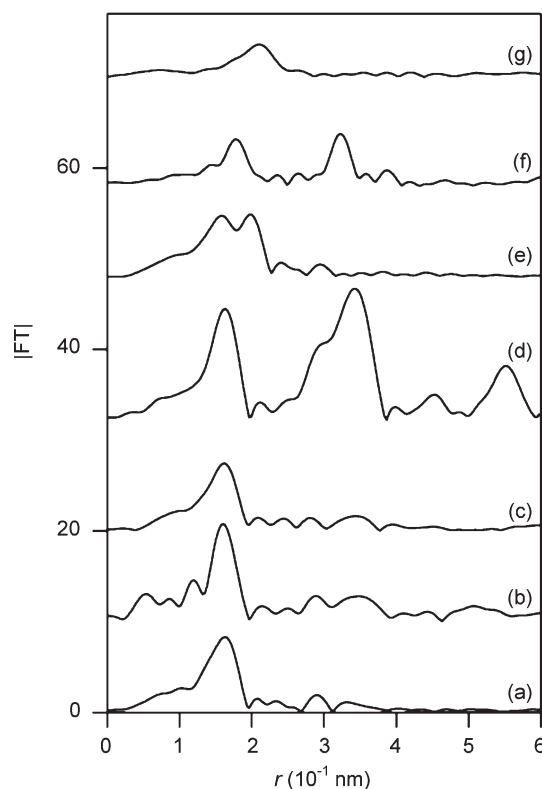


**Fig. 5** FT of  $k^3$ -weighted Sn K-edge EXAFS for (a)  $\text{Sn}(0.19)/\text{TN}$ , (b)  $\text{Sn}(0.40)/\text{TN}$ , (c)  $\text{Sn}(0.77)/\text{TN}$ , (d)  $\text{SnO}_2$ , (e)  $\text{SnCl}_4 \cdot 5\text{H}_2\text{O}$ , (f)  $\text{SnO}$ , and (g)  $\text{SnCl}_2 \cdot 2\text{H}_2\text{O}$ .

shown in Fig. 5. For the TN-intercalated Sn catalysts, the Sn–Cl bond peak at approximately 0.21 nm was not observed (Fig. 5a–c). Furthermore, the peaks observed for the  $\text{SnO}$  or  $\text{SnO}_2$  corresponding to the Sn–(O)–Sn bond were not observed in the second coordination sphere (Fig. 5d–g). Thus, aggregated Sn species, such as  $\text{SnO}$  or  $\text{SnO}_2$ , are not present in the TN interlayers.

In the case of TN-intercalated Sn catalysts, the peak in the range of ca. 0.1–0.2 nm in Fig. 5a was well fitted by using the Sn–O shell parameters.<sup>17</sup> The curve-fitting analysis of the  $\text{Sn}(0.19)/\text{TN}$  catalyst suggested that five oxygen atoms at 0.205 nm were coordinated to the monomeric  $\text{Sn}^{\text{IV}}$  centre (Table 2).<sup>18</sup> The distances from the Sn atoms to the nearest

**Table 2** Curve-fitting results of Sn K-edge EXAFS for various TN-intercalated Sn catalysts<sup>a</sup>

Sample	Shell	CN <sup>c</sup>	<i>R</i> (nm) <sup>d</sup>	$\sigma$ (nm) <sup>e</sup>
$\text{SnO}_2$ <sup>b</sup>	Sn–O	(6)	(0.206)	
	Sn–(O)–Sn	(2)	(0.318)	
	Sn–(O)–Sn	(8)	(0.371)	
$\text{Sn}(0.19)/\text{TN}$	Sn–O	5.4	0.205	0.0077
$\text{Sn}(0.40)/\text{TN}$	Sn–O	4.6	0.205	0.0055
$\text{Sn}(0.77)/\text{TN}$	Sn–O	4.8	0.206	0.0079

<sup>a</sup> Curve-fitting analysis was performed in  $k$ -space with the inverse FT of the 0.092 nm <  $r$  < 0.196 nm range using  $\text{SnO}_2$  as a standard material. <sup>b</sup> Data from X-ray crystallography. <sup>c</sup> Coordination number. <sup>d</sup> Bond distance. <sup>e</sup>  $\sigma$  is Debye–Waller factor.

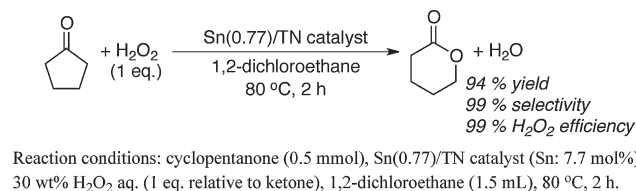
oxygen atoms were essentially consistent with the values determined by X-ray crystallography for the Sn–O bond ( $R = 0.206$  nm) in  $\text{SnO}_2$ .<sup>19</sup> Based on the results of the  $^7\text{Li}$  and  $^{119}\text{Sn}$  MAS NMR and Sn K-edge XAFS, we propose that the local structure of the Sn species in the TN interlayers is an isolated  $[\text{Sn}^{\text{IV}}(\text{OH})_x(\text{H}_2\text{O})_{5-x}]^{(4-x)+}$  ( $x = 0-3$ ) species.

To investigate the catalytic abilities of the  $\text{Sn}(0.77)/\text{TN}$ , the Baeyer–Villiger oxidation of cyclopentanone with aqueous  $\text{H}_2\text{O}_2$  at  $80^\circ\text{C}$  was carried out as a model reaction. It is noteworthy that the use of  $0.05$  g of the  $\text{Sn}(0.77)/\text{TN}$  catalyst (Sn content:  $0.0385$  mmol) in 1,2-dichloroethane (1,2-DCE:  $1.5$  mL) allowed cyclopentanone ( $0.5$  mmol) to react with aqueous  $\text{H}_2\text{O}_2$  (2 eq. relative to the ketone) in a highly effective manner, giving a quantitative yield of  $\delta$ -valerolactone in 2 h (Table 3, entry 1).<sup>20</sup> No oxidation proceeded in the absence of the catalyst or in the presence of the Li/TN catalyst. The  $\text{Sn}(0.77)/\text{TN}$  catalyst showed a high performance for oxidising various ketones using  $\text{H}_2\text{O}_2$  as the sole oxidant, as is summarised in Table 3. Cyclohexanone and 4-methyl cyclohexanone were converted to the corresponding lactones, such as  $\epsilon$ -caprolactone and  $\gamma$ -methyl- $\epsilon$ -caprolactone, respectively, with an excellent yield (entries 4 and 5). Sterically hindered 2-adamantanone and aliphatic 4-methyl-2-pentanone also acted as good substrates, giving a quantitative yield of 4-oxahomoadamantane-5-one and a 72% yield of 2-methylpropyl acetate, respectively (entries 6 and 7). After the oxidation, the spent  $\text{Sn}(0.77)/\text{TN}$  catalyst was easily separated by simple filtration. The recovered catalyst could be reused without additional treatment, and its high activity and selectivity were maintained (entries 2 and 3).<sup>21</sup> The amount of Sn species that leached into the reaction solution was sufficiently small to be undetectable by ICP analysis. To further demonstrate the requirement of the heterogeneous  $\text{Sn}(0.77)/\text{TN}$  catalyst, the solid

catalyst was removed by hot filtration after the oxidation of cyclopentanone reached almost 50% conversion. After removal of the catalyst, the reaction was monitored for 120 min, and additional formation of  $\delta$ -valerolactone was not observed.<sup>9</sup> These results show that the reaction proceeds on the TN interlayer and that leaching of the dissolved Sn species does not occur under the reaction conditions.

The most notable feature of catalytic Baeyer–Villiger oxidation with  $\text{H}_2\text{O}_2$  mediated by  $\text{Sn}(0.77)/\text{TN}$  was that cyclopentanone was able to be transformed into  $\delta$ -valerolactone specifically with 99% selectivity and 99% efficiency with respect to  $\text{H}_2\text{O}_2$  utilisation, as highlighted in Scheme 1.

The effect of the Sn loading amount on the Baeyer–Villiger oxidation of cyclopentanone using various TN-intercalated Sn catalysts was explored (Table 4). The catalytic activity increased as the loading amount of Sn decreased, despite the narrow CS. The  $\text{Sn}(0.19)/\text{TN}$  catalyst showed the highest catalytic activity, and only  $\delta$ -valerolactone, in an almost quantitative yield, was formed (entry 3). Among the other Sn compounds examined as catalysts,  $\text{SnO}$ ,  $\text{SnO}_2$ ,  $\text{Sn}(\text{OH})_4$ ,  $\text{SnCl}_2 \cdot 2\text{H}_2\text{O}$ , and  $\text{SnCl}_4 \cdot 5\text{H}_2\text{O}$  were not effective at all under the same reaction conditions (entries 4–8).



Scheme 1

Table 3 Substrate screening for  $\text{Sn}(0.77)/\text{TN}$ -catalysed Baeyer–Villiger oxidation<sup>a</sup>

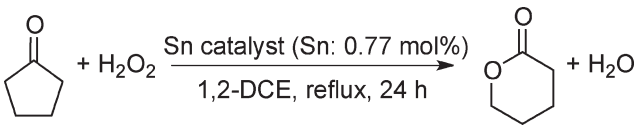
Entry	Substrate	Time (h)	Product	Conv. (%) <sup>b</sup>	Yield (%) <sup>b</sup>
1		2		100	>99 (89)
2 <sup>c</sup>		2		99	98
3 <sup>d</sup>		2		97	97
4		10		100	>99 (78)
5		6		98	98 (93)
6		6		98	>99 (81)
7		6		77	72

<sup>a</sup> Substrate ( $0.5$  mmol),  $\text{Sn}(0.77)/\text{TN}$  catalyst ( $0.05$  g, Sn:  $7.7$  mol%), 1,2-DCE ( $1.5$  mL),  $30$  wt%  $\text{H}_2\text{O}_2$  (2 eq. relative to the ketone), reflux.

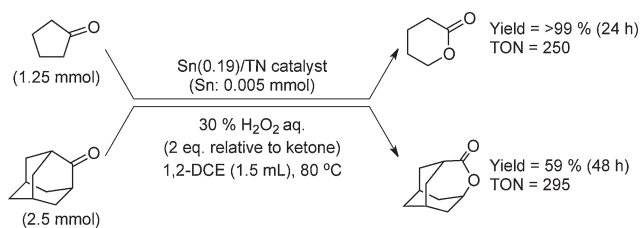
<sup>b</sup> Determined by GC using an internal standard technique. Values in parentheses were isolated yields. <sup>c</sup> 1st recycle. <sup>d</sup> 2nd recycle.



**Table 4** Baeyer–Villiger oxidation with various TN-intercalated Sn catalyst<sup>a</sup>

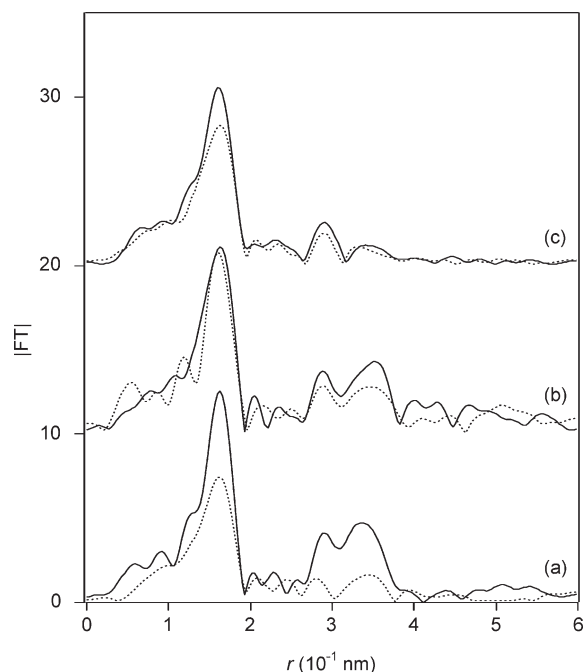
				
Entry	Catalyst	CS (nm) <sup>b</sup>	Conv. (%) <sup>c</sup>	Yield (%) <sup>c</sup>
1	Sn(0.77)/TN	0.55	79	75
2	Sn(0.40)/TN	0.52	90	85
3	Sn(0.19)/TN	0.27	100	>99
4	SnCl <sub>4</sub> ·5H <sub>2</sub> O	—	trace	n.d. <sup>d</sup>
5	SnCl <sub>2</sub> ·2H <sub>2</sub> O	—	trace	n.d. <sup>d</sup>
6	Sn(OH) <sub>4</sub>	—	trace	n.d. <sup>d</sup>
7	SnO <sub>2</sub>	—	trace	n.d. <sup>d</sup>
8	SnO	—	trace	n.d. <sup>d</sup>

<sup>a</sup> Cyclopentanone (0.7 mmol), Sn catalyst (Sn: 0.77 mol% of substrate), 1,2-DCE (1.5 mL), 30 wt% H<sub>2</sub>O<sub>2</sub> (2 eq. relative to ketone), reflux, 24 h. <sup>b</sup> Calculated from XRD profiles. <sup>c</sup> Determined by GC using an internal standard technique. <sup>d</sup> Not detected.

**Scheme 2**

In the case of cyclopentanone as a substrate, the Sn(0.19)/TN catalyst showed a high turnover number (TON; moles of product per mole of Sn content) of 250, as demonstrated in Scheme 2. This TON value of the Sn(0.19)/TN catalyst is the highest reported for a Sn-containing heterogeneous catalyst system to date. Other TON values include the following: 48 for Sn-β-zeolite,<sup>5a</sup> 63 for Sn/hydrotalcite,<sup>6c</sup> 132 for Sn/palygorskite,<sup>6f</sup> 58 for Sn/polystyrene,<sup>6d</sup> 9 for Sn-dendrimer/polystyrene,<sup>6a</sup> 4 for Sn-dendrimer/cellulose,<sup>6c</sup> and 75 for Sn/montmorillonite.<sup>6g</sup> Furthermore, the highest TON value to date, 295, was also obtained in the 2-adamantanone oxidation in the presence of the Sn(0.19)/TN catalyst; other TON values include the following: 145 for Sn-β-zeolite,<sup>5a</sup> 173 for Sn-MCM-41,<sup>6b</sup> 164 for Sn/palygorskite,<sup>6f</sup> 215 for Sn/polystyrene,<sup>6d</sup> 28 for Sn-dendrimer/polystyrene,<sup>6a</sup> 4 for Sn-dendrimer/cellulose,<sup>6c</sup> and 166 for Sn/montmorillonite.<sup>6g</sup>

After the reaction, the XRD profiles of the recovered TN-supported Sn catalysts revealed that the recovered catalyst had almost the same layered structure as the fresh catalyst.<sup>9</sup> The FT of the *k*<sup>3</sup>-weighted Sn K-edge EXAFS data for the recovered TN-intercalated Sn catalysts is shown in Fig. 6.<sup>22</sup> In the second coordination sphere of recovered Sn(0.77)/TN and recovered Sn(0.40)/TN, however, the peak at approximately 0.35 nm corresponding to the Sn–(O)–Sn bond was detected because of the formation of an aggregated species such as SnO<sub>2</sub> (Fig. 6a and 6b). In contrast, the Sn<sup>IV</sup> species in the Sn(0.19)/TN interlayer maintained its monomeric structure even after the oxidation reaction (Fig. 6c). Based on the above results, it can be concluded

**Fig. 6** FT of Sn K-edge EXAFS spectra for (a) Sn(0.77)/TN, (b) Sn(0.44)/TN, and (c) Sn(0.19)/TN catalyst. The solid curves are recovered catalysts, and the dashed curves are fresh catalysts.

that the highly dispersed monomeric [Sn<sup>IV</sup>(OH)<sub>x</sub>(H<sub>2</sub>O)<sub>5-x</sub>]<sup>(4-x)+</sup> (*x* = 0–3) species in the TN interlayer can act as an effective active species for this reaction.

## Conclusions

Isolated [Sn<sup>IV</sup>(OH)<sub>x</sub>(H<sub>2</sub>O)<sub>5-x</sub>]<sup>(4-x)+</sup> (*x* = 0–3) species were able to intercalate into the TN interlayers, as confirmed by XRD, <sup>7</sup>Li MAS NMR, <sup>119</sup>Sn MAS NMR, and Sn K-edge XAFS analyses. Sn(0.19)/TN is an effective heterogeneous catalyst for the Baeyer–Villiger oxidation of various cyclic ketones with excellent TON values. No Sn leaching was observed during the oxidations, and the catalyst was recyclable. We expect that our intercalation protocol based on TN as a cation-exchanger will offer an attractive route for the design of functional catalysts at the atomic and molecular levels.

## Experimental section

### General

All organic chemical compounds were purified by standard procedures before use. Analytical GLC was performed by a Shimadzu GC-8A with a flame ionization detector equipped with Thermo 3000 and Silicone OV-101 packing. GC-MS was performed by a Shimadzu GC-17B with a thermal conductivity detector equipped with an RT-βDEXsm capillary column. <sup>1</sup>H and <sup>13</sup>C NMR spectra were obtained on JNM-AL400 or spectrometers at 400 MHz in chloroform-*d*<sub>1</sub> with TMS as an internal standard. Products were confirmed by the comparison of their GC retention time, mass, <sup>1</sup>H and <sup>13</sup>C NMR spectra with those of authentic samples. Data of XRD measurement were recorded on

a MAC Science MXP<sup>3</sup>V in reflection mode at 25 kV and 10 mA using Cu-K $\alpha$  radiation ( $\alpha_1 = 0.154057$  nm,  $\alpha_2 = 0.154433$  nm, weighted average = 0.154178 nm). The samples were loaded on glass plate sample holders whose reflections did not interfere with their characterization. Infrared spectra were obtained with a HORIBA FT-720. Samples were diluted with KBr and compressed into thin disk shaped pellets. Spectra were taken in transmission mode over the range of 400–4000 cm<sup>-1</sup>, with 16 scans at 4 cm<sup>-1</sup> resolutions. ICP measurements were performed on SPS 1800H Plasma Spectrometer by SII (Sn element: 189.898 nm). The <sup>7</sup>Li nuclear magnetic resonance spectra were acquired using a superconducting magnet (600 MHz, JEOL ECA-600). The sample rotor of zirconia (4.0 mm) was spun at the spinning frequency of 15 kHz. The measurement of NMR spectra was performed using the non-decoupling single-pulse method. Chemical shifts were referenced to 1.0 mol L<sup>-1</sup> of aqueous LiCl as an external standard (0 ppm). The <sup>119</sup>Sn nuclear magnetic resonance spectra were acquired using a superconducting magnet (223.81 MHz, JEOL ECA-600). The sample rotor of zirconia (3.2 mm) was spun at the spinning frequency of 20 kHz. The measurement of NMR spectra was performed using the non-decoupling single-pulse method. Chemical shifts were references to (CH<sub>3</sub>)<sub>4</sub>Sn as an external standard (0 ppm). X-ray absorption spectra around the Sn K-edges were recorded at the BL01B1 beamline of the SPring-8 (8 GeV, 100 mA) of the Japan Synchrotron Radiation Research Institute (Proposal No. 2010B1100 by Professor Dr Kiyotomi Kaneda, Graduate School of Engineering Science, Osaka University). A Si (311) two-crystal monochromator was used. Ion chambers filled with Ar(100%) and Ar(50%)/Kr(50%) were used for the *I*<sub>0</sub> and *I* detectors, respectively, and the samples were located between these ion chambers. Energy calibration was carried out using a Sn foil (30 mm of thickness). Sn K-edge XANES and EXAFS spectra of all samples were recorded in the step scan mode. Data reduction using the REX2000 Ver.2.3.3 program (Rigaku) was carried out. The EXAFS analysis was performed as described below. The spectra were extracted by utilizing the cubic spline method and normalized to the edge height. The *k*<sup>3</sup>-weighted EXAFS oscillation was Fourier transformed into *r* space, with the Fourier transformation range between 3.0 and 16.0 Å<sup>-1</sup>. The amount of hydrogen peroxide was determined by titration method by use of KMnO<sub>4</sub>.

### Preparation of TN-intercalated Sn catalysts

The intercalation of Sn species into TN interlayer was achieved by the following procedure. Into a round-bottomed flask with Li/TN (1 g), deionized water (10 mL) and methanol (10 mL) were added, and then the mixture was stirred to swell at room temperature. After 1 h, SnCl<sub>2</sub>·2H<sub>2</sub>O (0.15 g: 50% of CEC) in methanol (30 mL) was added, followed by the addition of deionized water (30 mL), and stirred at 30 °C for 48 h. The obtained slurry was filtered, washed with deionized water, and dried under vacuum overnight. The same intercalation procedure by use of the above Sn-containing TN, was repeated two times, TN-intercalated Sn catalyst, Sn(0.77)/TN, was obtained. To control the loading amount of Sn species, the Sn amount was changed to 0.08 g × 2 times or 0.038 g × 2 times in the intercalation

procedure. The obtained TN-intercalated Sn catalyst were abbreviated as (0.40)/TN and Sn(0.19)/TN, respectively.

### Typical procedure for Baeyer–Villiger oxidation

Into a Schlenk tube with a reflux condenser was placed cyclopentanone (0.5 mmol), Sn catalyst (Sn: 7.7 mol%), 1,2-dichloroethane (1.5 mL), and 30 wt% H<sub>2</sub>O<sub>2</sub> (2 eq. relative to ketone). The resulting mixture was refluxed for 24 h. Cyclopentanone conversion and lactone yields were periodically determined by GC analysis. After 24 h, the Sn(0.77)/TN catalyst was separated by a filtration. The filtrate was treated with MnO<sub>2</sub>, followed by extraction with diethyl ether. The solvent was removed *in vacuo*, and the residue was purified *via* bulb-to-bulb distillation or sili-cagel column chromatography. Analytically pure  $\delta$ -valerolactone (0.0445 g, 89%) was obtained.

### Acknowledgements

This study was supported by a Grant-in-Aid for Scientific Research from the Ministry of Education, Culture, Sports, Science, and Technology of Japan (19560771). Some of the experiments were carried out at the BL01B1 beamline of the SPring-8 of the Japan Synchrotron Radiation Research Institute (Proposal No. 2010B1100).

### References

- 1 A. Baeyer and V. Villiger, *Ber. Dtsch. Chem. Ges.*, 1899, **32**, 3625.
- 2 G. R. Krow, *Org. React.*, 1993, **43**, 251.
- 3 For review, see (a) M. Renz and B. Meunier, *Eur. J. Org. Chem.*, 1999, 737; (b) G. Strukul, *Angew. Chem., Int. Ed.*, 1998, **37**, 1198; (c) G.-J. ten Brink, I. W. C. E. Arends and R. A. Sheldon, *Chem. Rev.*, 2004, **104**, 4105.
- 4 C. Jiménez-Sanchidrián and J. R. Ruiz, *Tetrahedron*, 2008, **64**, 2011.
- 5 (a) A. Corma, L. T. Nemeth, M. Renz and S. Valencia, *Nature*, 2001, **412**, 423; (b) M. Renz, T. Blasco, A. Corma, V. Fornés, R. Jensen and L. T. Nemeth, *Chem.–Eur. J.*, 2002, **8**, 4708; (c) S. R. Bare, S. D. Kelly, W. Sinkler, J. J. Low, F. S. Modica, S. Valencia, A. Corma and L. T. Nemeth, *J. Am. Chem. Soc.*, 2005, **127**, 12924; (d) M. Boronat, A. Corma, M. Renz, G. Sastre and P. M. Viruela, *Chem.–Eur. J.*, 2005, **11**, 6905; (e) M. Boronat, P. Concepción, A. Corma and M. Renz, *Catal. Today*, 2007, **121**, 39.
- 6 (a) Q.-G. Zhang, S.-X. Wen and Z.-Q. Lei, *React. Funct. Polym.*, 2006, **66**, 1278; (b) A. Corma, M. T. Navarro, L. T. Nemeth and M. Renz, *Chem. Commun.*, 2001, 2190; (c) C.-L. Li, J.-Q. Wang, Z.-W. Yang, Z.-G. Hu and Z.-Q. Lei, *Catal. Commun.*, 2007, **8**, 1202; (d) J.-Q. Wang, R.-R. Wang, Z. Zhang, C.-L. Li, Z.-W. Yang and Z.-Q. Lei, *J. Macromol. Sci., Part A: Pure Appl. Chem.*, 2008, **45**, 672; (e) U. R. Pillai and E. Sahle-Demessie, *J. Mol. Catal. A: Chem.*, 2003, **191**, 93; (f) Z.-Q. Lei, Q.-H. Zhang, J.-J. Luo and X.-Y. He, *Tetrahedron Lett.*, 2005, **46**, 3505; (g) Z.-Q. Lei, G.-F. Ma and C.-G. Jia, *Catal. Commun.*, 2007, **8**, 305; (h) A. Corma, M. T. Navarro and M. Renz, *J. Catal.*, 2003, **219**, 242; (i) M. Boronat, P. Concepción, A. Corma, M. T. Navarro, M. Renz and S. Valencia, *Phys. Chem. Chem. Phys.*, 2009, **11**, 2876.
- 7 H. Toraya, S. Iwai, F. Marumo and H. Hirao, *Z. Kristallogr.*, 1977, **146**, 73.
- 8 (a) T. Sento, S. Shimazu, N. Ichikuni and T. Uematsu, *Chem. Lett.*, 1998, **27**, 1191; (b) S. Shimazu, M. Suzuki, N. Ichikuni and T. Uematsu, *J. Ion Exchange*, 2003, **14**, 397; (c) N. Yamaguchi, S. Shimazu, N. Ichikuni and T. Uematsu, *Chem. Lett.*, 2004, **33**, 208; (d) Y. Permana, S. Shimazu, N. Ichikuni and T. Uematsu, *J. Mol. Catal. A: Chem.*, 2004, **221**, 141; (e) S. Shimazu, H. Zou, T. Hara and N. Ichikuni, *J. Ion Exchange*, 2007, **18**, 584.
- 9 Data are shown in ESI†.

- 10 R. K. Harris, B. E. Mann, *NMR and the Periodic Table*, Academic Press, London, 1978.
- 11 P. Porion, A. M. Faugère and A. Delville, *J. Phys. Chem. C*, 2008, **112**, 9808.
- 12 The same results are obtained in the characterisation of Na/TN, K TN<sup>-1</sup>, and Ca/TN by use of <sup>7</sup>Li MAS NMR, as also shown in ESI†.
- 13 P. J. Smith and A. P. Tupciauskas, *Annu. Rep. NMR Spectrosc.*, 1978, **8**, 291.
- 14 *Multinuclear Solid-State NMR of Inorganic Materials*, Pergamon Materials Series, ed. K. J. D. MacKenzie, Pergamon, Amsterdam, 2002, vol. 6.
- 15 B. Wrackmeyer, *Annu. Rep. NMR Spectrosc.*, 1995, **16**, 73.
- 16 C. Cossement, J. Darville, J.-M. Gilles, J. B. Nagy, C. Fernandez and J.-P. Amoureux, *Magn. Reson. Chem.*, 1992, **30**, 263.
- 17 Curve-fitting analysis was performed for the Sn–O shell with the range of the Sn–O shell being between 0.092 and 0.196 nm. The Sn–O phase and amplitude functions were extracted from SnO<sub>2</sub>, which has a rutile tetragonal lattice *P4<sub>2</sub>/mnm*.
- 18 Since it is hard to discriminate between Sn–OH or Sn–(OH<sub>2</sub>) bond from Sn K-edge XAFS analysis, the each coordination number of Sn–OH or Sn–(OH<sub>2</sub>) bond can not be provided.
- 19 M. Intissar, J.-C. Jumas, J.-P. Besse and F. Leroux, *Chem. Mater.*, 2003, **15**, 4625.
- 20 Following the screening of solvent for Baeyer–Villiger oxidation, the highest catalytic activity was obtained in 1,2-dichloroethane solvent, shown in ESI†.
- 21 After the third and forth recycling experiment of Sn(0.77)/TN catalysed Baeyer–Villiger oxidation, the yields of  $\delta$ -valerolactone were 92% and 88%, respectively.
- 22 Sn K-edge XANES spectra of the recovered catalysts are also shown in the ESI†.